analytical chemistry

pubs.acs.org/ac Article

High-Speed Screening of Lipoprotein Components Using Online Miniaturized Asymmetrical Flow Field-Flow Fractionation and Electrospray Ionization Tandem Mass Spectrometry: Application to Hepatocellular Carcinoma Plasma Samples

Jin Yong Kim, Gwang Bin Lee, Jong Cheol Lee, and Myeong Hee Moon*

Cite This: *Anal. Chem.* 2021, 93, 4867−4875 Read Online

ACCESS | Metrics & More | Article Recommendations | Supporting Information

ABSTRACT: This study introduces a high-speed screening method for the quantitative analysis of lipoprotein components in human plasma samples using online miniaturized asymmetrical flow field-flow fractionation and electrospray ionization-tandem mass spectrometry (mAF4-ESI-MS/MS). Using an mAF4 channel, high-density lipoproteins and low-density lipoproteins can be fractionated by size at a high speed (<10 min) and directly fed to ESI-MS/MS for the simultaneous screening of targeted lipid species and apolipoprotein A1 (ApoA1). By employing the heated electrospray ionization probe as an ionization source, an mAF4 effluent flow rate of up to a few tens of microliters per minute can be used, which is adequate for direct feeding to MS without splitting the outflow, resulting in a consistent feed rate to MS for stable MS detection. mAF4-ESI-MS/MS was applied to hepatocellular carcinoma (HCC) plasma samples for targeted quantification of 25 lipid biomarker candidates and ApoA1 compared with healthy controls, the results of which were in statistical agreement with the quantified results obtained by nanoflow ultrahigh performance liquid chromatography−tandem mass spectrometry. Moreover, the present method provided the simultaneous detection of changes in lipoprotein size and the relative amount. This study demonstrated the potential of mAF4-ESI-MS/MS as an alternative high-speed screening platform for the top-down analysis of targeted lipoprotein components in patients with HCC, which is applicable to other diseases that involve the perturbation of lipoproteins.

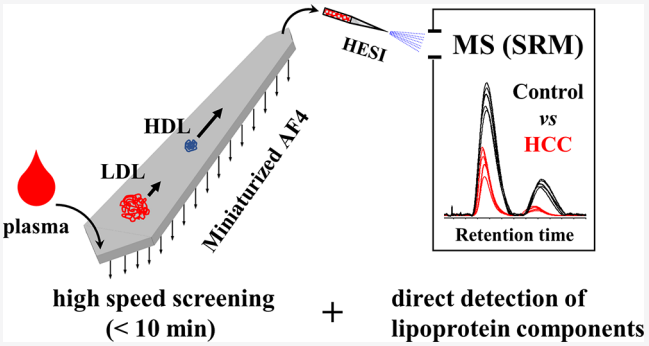

INTRODUCTION

Lipids are one of the most abundant classes of cellular metabolites and play important roles in various metabolic processes, such as energy storage and supply, signaling, cell proliferation and death, and the construction of cellular membranes.[1−3] In particular, lipid interaction with specific proteins is well known because lipids and proteins form complexes in an aqueous biological system environment to function as nuclear receptors or lipid transporters.[4,5] Lipoproteins, which are composed of lipids and proteins, are the most representative complexes in the blood system and are mainly involved in the transportation of lipids and cholesterols through the blood vessels.[6] Lipoproteins are classified into several subclasses based on their densities, including high-density lipoproteins (HDL), low-density lipoproteins (LDL), and very-low-density lipoproteins. Some apolipoproteins are considered markers of specific lipoproteins because they are present exclusively in specific lipoprotein subclasses.[7] For example, apolipoprotein A1 (ApoA1) is the major structural protein component of HDL and is rarely present in other lipoprotein subclasses. To date, the biological roles of apolipoproteins and lipids associated with the development of cardiovascular diseases, such as atherosclerosis and coronary artery disease (CAD), have been well investigated; however, their pathogenic association with cancer has scarcely been explored.[8−11]

As a whole blood sample is often used as a source of metabolites in most studies related with disease diagnosis, the clinical significances and features of a change in the relative amount of lipids and associating proteins in lipoprotein subclasses have not been examined thoroughly.[12] Few separation/isolation methods have been utilized to isolate different types of lipoproteins from blood plasma or serum

Received: November 11, 2020
Accepted: February 26, 2021
Published: March 10, 2021

https://dx.doi.org/10.1021/acs.analchem.0c04756
Anal. Chem. 2021, 93, 4867−4875

samples: density gradient ultracentrifugation, size exclusion chromatography, and gel electrophoresis.[13−16] However, chromatographic or gel-based separation methods generally require long processing times in extracting and purifying lipoproteins and are associated with the possibility of sample loss in the stationary phase or gel matrix.

Flow field-flow fractionation (FlFFF) can be an alternative for separating biological macromolecules, such as proteins, exosomes, subcellular species, cells, and lipoproteins, without the above drawbacks.[17−23] FlFFF is an elution-based separation method capable of fractionating particles or macromolecules by size within an unobstructed channel space with the use of two different flow streams: the migration flow that carries sample components along the channel toward the detector and the cross-flow that moves across the channel to force sample materials toward the channel wall, resulting in the retardation of their migration.[24,25] As FlFFF utilizes an empty channel space, the possibility of sample loss or shear degradation, which can often be caused by packing materials or gel matrices, can be avoided. Moreover, biological components can be treated in their intact forms without being denatured or dissociated owing to the use of aqueous carrier liquids, including biological buffer solutions. The detection capability of FlFFF has been empowered by direct hybridization with multi-angle light scattering for the calculation of accurate molecular weight (MW) and the conformation information of macromolecules.[26] More recently, FlFFF has been applied to the top-down analysis of metalloproteins in blood plasma and lipids in plasma lipoproteins by direct coupling with inductively coupled plasma mass spectrometry and electrospray ionization-tandem mass spectrometry (ESI-MS/MS), respectively, based on the use of a miniaturized FlFFF channel, which can be operated under reduced flow rate conditions.[27−29]

In this study, a miniaturized asymmetrical FlFFF (mAF4) channel coupled with ESI-MS/MS was employed for the targeted analysis of lipids and proteins of lipoproteins derived from human liver cancer (hepatocellular carcinoma, HCC) plasma samples. The mAF4-ESI-MS/MS system not only fractionates different lipoproteins by size but also analyzes lipid species and apolipoproteins in lipoproteins by top-down lipidomic and proteomic quantitation. Moreover, mAF4-ESI-MS/MS is advantageous for the top-down lipoprotein analysis as the speed of analysis can be enhanced with the bypass of lipid extraction or other sample preparation, and a minimal loss of lipoprotein conformation can be minimized with the use of biological buffer, which is suitable for the targeted analysis of lipoprotein components directly. The feed rate of the previous top-down lipidomic approach using mAF4-ESI-MS/MS was based on splitting the outflow in order to reduce the feed rate to ESI-MS and was relatively unstable.[27] The present study employs a heated electrospray ionization (HESI) probe, which enhances the desolvation of an aqueous FlFFF effluent.[30] With HESI, the mAF4 effluent can be used up to tens of μL/min without splitting the outflow and making it beneficial for maintaining a stable feed rate to ESI-MS, with stability in repeated measurements. The method introduced here was applied to HCC patients' plasma samples for the direct analysis of ApoA1 and 25 lipid molecules that were previously reported to exhibit significant changes in patients with liver cancer compared with healthy controls.[31] For confirmation, targeted quantification of 25 lipid species in lipoproteins was conducted with the same samples at each lipoprotein level using nanoflow ultrahigh performance liquid chromatography−tandem mass spectrometry (nUHPLC-ESI-MS/MS) based on selected reaction monitoring (SRM), and the results from the two analytical methods were statistically compared.

EXPERIMENTAL SECTION

Materials and Reagents. Ammonium bicarbonate (NH_4HCO_3), formic acid (HCO_2H), ammonium hydroxide (NH_4OH), ammonium formate (NH_4HCO_2), four protein standards [carbonic anhydrase (CA), bovine serum albumin, apoferritin, and thyroglobulin], two lipoprotein standards (HDL and LDL), and ProteoPrep Immunoaffinity Albumin & IgG Depletion kit were purchased from Sigma-Aldrich (St. Louis, MO, USA). High-performance liquid chromatography (HPLC)-grade solvents [H_2O, CH_3CN, CH_3OH, isopropanol, and methyl-*tert*-butyl ether (MTBE)] were purchased from J.T. Bakers (Philipsburg, NJ, USA). Fused-silica capillaries used for preparing capillary LC columns and tubing connections were obtained from Polymicro Technology LCC (Phoenix, AZ, USA): 50, 75, and 100 μm i.d.; 365 μm o.d. for all. All the fittings, unions, and PEEK tubing for mAF4 were purchased from Upchurch Scientific of IDEX Health & Science, LCC (Oak Harbor, WA, USA). Lipid standards (Avanti Polar Lipids Inc., Alabaster, AL, USA) with odd-numbered or deuterated acyl chains were used as internal standards (ISs) and were added to the plasma lipid extract for SRM quantitation using nUHPLC-ESI-MS/MS: lysophosphatidylcholine (LPC) 18:1-D_7, phosphatidylcholine (PC) 15:0/18:1-D_7, lysophosphatidylethanolamine (LPE) 18:1-D_7, phosphatidylethanolamine (PE) 15:0/18:1-D_7, lysophosphatidic acid (LPA) 17:0, phosphatidic acid (PA) 15:0/18:1-D_7, phosphatidylglycerol (PG) 15:0/18:1-D_7, lysophosphatidylinositol (LPI) 13:0, phosphatidylinositol (PI) 15:0/18:1-D_7, sphingomyelin (SM) d18:1/18:1-D_9, ceramide (Cer) d18:0-D_7/24:0, monohexosylceramide (MHC) d18:1-D_7/15:0, diacylglycerol (DG) 15:0/18:1-D_7, and triacylglycerol (TG) 15:0/18:1-D_7.

Human Plasma Samples. Plasma samples from healthy controls (age = 46.4 ± 2.1 years, n = 10) were provided by the Ajou University Hospital Biobank (Suwon, Korea) through the Korea Bioresources Network under written consent from the Institutional Review Board (IRB). Plasma samples from patients with HCC (age = 53.0 ± 5.7 years, n = 10) were obtained under written consent from the IRB of the Biobank of Severance Hospital (Seoul, Korea). This study was conducted in accordance with the current version of the Declaration of Helsinki. All the samples used were from male participants to rule out the possible hormonal effects on the regulation of blood lipid metabolites.[32] Demographic data of the participants are listed in Table S1. All the samples were stored at −80 °C until use. ProteoPrep Immunoaffinity depletion kit was used to deplete the plasma samples of albumin and IgG prior to FlFFF analysis, based on the manufacturer's instructions. The protein concentration of each depleted sample was measured based on the Bradford assay, using Coomassie Brilliant Blue G-250 from Bio-Rad Laboratories, Inc. (Hercules, CA, USA).

mAF4-ESI-MS/MS. The mAF4 channel utilized in this study was assembled as previously described,[33] and details of the mAF4 channel are provided in the Supporting Information. A model SP930D HPLC pump from Young-Lin Instruments (Seoul, Korea) was utilized for delivering the carrier solution to the mAF4 channel. The carrier solution for mAF4

https://dx.doi.org/10.1021/acs.analchem.0c04756
Anal. Chem. 2021, 93, 4867−4875

separation was 10 mM ammonium bicarbonate (NH_4HCO_3) solution prepared with ultrapure water (>18 MΩ·cm) and filtered through a nitrocellulose membrane filter (0.22 μm) from Millipore (Danvers, MA, USA). The sample was injected into the mAF4 channel through the model 7725i loop injector (Rheodyne, Cotati, CA, USA) at a flow rate of 400 μL/min in the focusing/relaxation stage (dotted lines in Figure 1), in

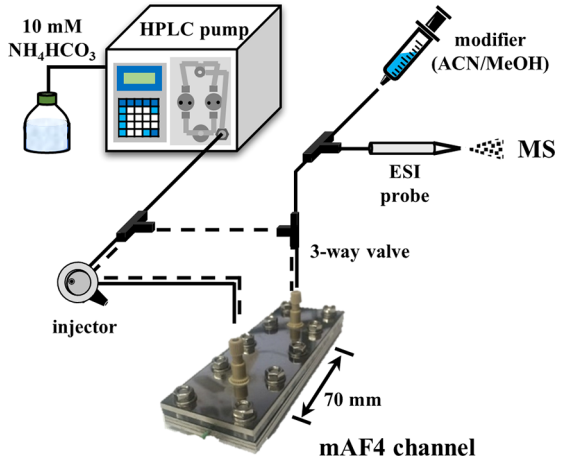

Figure 1. Schematic of online mAF4-ESI-MS/MS system for lipoprotein analysis from human plasma.

which two flow streams through the inlet and outlet were focused at a 1/10 position from the channel inlet by converting to three-way valves. Salts and impurities smaller than the membrane pore size (MWCO 10 kDa) were expected to be discharged via the cross-flow. During the elution mode (solid lines in Figure 1), the outflow from the mAF4 channel outlet was set to 25 μL/min by adjusting the length of a narrow-bore capillary tube. The outflow was merged with the modifier flow (varied from 5 to 35 μL/min) from a syringe pump via a MicroTee, resulting in the final rates of 30−60 μL/min fed to the MS column. The ionization modifier solutions were ACN/MeOH (5:5, v/v) with 1.0% HCO_2H in the positive ion mode and 0.5% NH_4OH in the negative ion mode of MS detection.

For mAF4-ESI-MS/MS analysis, the mAF4 channel was directly interfaced with an LTQ Velos ion trap mass spectrometer (Thermo Scientific, San Jose, CA, USA) via a HESI-II probe. The operating conditions of ESI-MS were as follows: 15 psi of sheath gas (N_2) pressure, 5 arbitrary units of auxiliary gas (N_2) flow rate, 3.0 kV of ESI voltage, ion transfer tube temperature of 300 °C, 40 eV of in-source fragmentation, and 40% of collision energy.

Lipid Analysis by nUHPLC-ESI-MS/MS. Lipid extraction from plasma samples followed the optimized extraction using MTBE/MeOH.[34,35] The details of lipid extraction are provided in the Supporting Information. nLC-ESI-MS/MS analysis for plasma lipids was accomplished using a binary LC pump, a Dionex Ultimate 3000 RSLCnano UPLC system (Thermo Scientific, San Jose, CA, USA), interfaced with an LTQ Velos ion trap mass spectrometer with a lab-prepared capillary column. The capillary column was prepared with a pulled-tip capillary (7 cm × 100 μm i.d.) without a frit. A 0.5 cm portion of the column tip was packed with 3 μm Watchers ODS-P C18 particles (Isu Industry Corp., Seoul, Korea) as a self-assembled frit, and the remaining portion (6.5 cm) of the column was packed with 1.7 μm XBridge BEH C18 130 Å particles (Waters, Milford, MA, USA) under nitrogen gas at 1000 psi. Mobile phase solutions for the binary gradient LC separation were (9:1, v/v) H_2O/CH_3CN for A and (2:2:6, v/v/v) CH_3OH/CH_3CN/IPA for B. Both solutions were added with 5 mM NH_4HCO_2 and 0.05% NH_4OH as a mixed ionization modifier for both positive and negative ion modes. Lipid samples were injected into the analytical column with 99% mobile phase A at a flow rate of 750 nL/min for 0.1 min. After sample loading, mobile phase B was increased to 75% over 5 min, 90% over 5 min, 99% over 15 min, and maintained at 99% for another 3 min at the same flow rate of 750 nL/min without splitting the flow. Thereafter, mobile phase B was decreased to 1%, and the analytical column was reconditioned for 7 min. The ESI voltage was set to 3.0 kV; the m/z ranges for the precursor scans were 250−1200 for both the positive and negative ion modes; and 40% of the normalized collision energy was applied with an isolation width of m/z 2 for data-dependent CID analysis. The targeted quantification of selected lipids was based on SRM analysis by measuring the peak area of a precursor ion and its specific product ions (Table S2). The lipid classes of LPC, PC, LPE, PE, DG, TG, SM, Cer, and MHC were detected in the positive ion mode, whereas the lipid classes of PG, LPA, PA, LPI, and PI were monitored in the negative ion mode. The base peak chromatograms (BPCs) obtained from the control and HCC patient groups, in both positive and negative ion modes, are shown in Figure S1 (Supporting Information). To compensate for the spectral fluctuation in MS intensity, 1 pmol each of the 14 lipid standards with odd-numbered or deuterium-substituted fatty acyl chains was injected into the plasma lipid extract samples as an IS. Targeted lipids (total 41 species) were quantified by calculating the corrected peak area, which is the ratio of the species peak area to that of the corresponding IS.

RESULTS AND DISCUSSION

The performance of the mAF4 channel is demonstrated by the separation of HDL and LDL standards (Figure 2a, top) and the separation of four protein standards (CA, BSA, apoferritin, and thyroglobulin) (Figure 2a, bottom), which were obtained with 1 μg of each standard at a flow rate of $\dot{V}_{out}/\dot{V}_c$ (outflow/cross-flow rates) = 0.025/0.475 mL/min and UV detection at 280 nm. The run conditions were adjusted to achieve a baseline separation of HDL and LDL standards within a relatively short analysis time (<10 min) for the high-speed screening of lipoprotein components from plasma samples. Under these run conditions, the separation of protein standards ranging from 29 to 669 kDa was achieved within 8.0 min, with some loss of resolution in separation (Figure 2a, bottom). Figure 2b shows the extracted ion fractogram (EIF) of a plasma sample based on the detection of PC 36:3 by mAF4-ESI-MS/MS. The fractogram in Figure 2b was generated by the SRM of PC 36:3 from plasma, which was obtained during the SRM transition of the precursor ion (m/z 784.5, $[M + H]^+$) to the phosphocholine ion (m/z 184.0, $[Pcho + H]^+$), which is a typical fragment ion resulting from the loss of phosphocholine head group ($HPO_4(CH_2)_2N(CH_3)_3$, 183 Da) during the CID experiment. Because of the detection of PC based on the loss of a phosphocholine head group, the chain structure of PC species from the mAF4-ESI-MS/MS run is expressed in the form of the total carbon number of acyl chains and the total number of double bonds as PC 36:3 instead of the individual acyl chain information as the R1/R2 form. The types of product ions used for detecting

https://dx.doi.org/10.1021/acs.analchem.0c04756
Anal. Chem. 2021, 93, 4867−4875

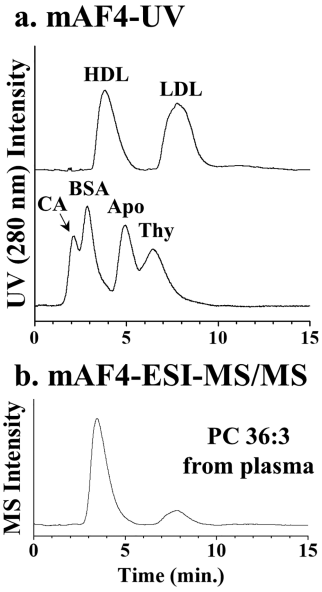

Figure 2. (a) Separation of the HDL and LDL standards (1 μg each, top) and the separation of four protein standards [CA (29 K); BSA, bovine serum albumin (66 K); Apo, apoferritin (444 K); Thy, thyroglobulin (669 K), bottom] using mAF4-UV at $\dot{V}_{out}/\dot{V}_c$ = 0.025/0.475 mL/min. (b) mAF4-ESI-MS/MS of human plasma sample represented with EIF of PC 36:3 SRM transition of m/z 784.5 ($[M + H]^+$) → m/z 184.0 ($[Pcho + H]^+$).

other lipids and proteins using mAF4-ESI-MS/MS analysis are listed in Table S2. The acyl chain structures of the PE and TG species are expressed in the same way as those of PC species. However, other lipid classes are expressed with the full chain structures because their acyl chain product ions are readily distinguished in the MS/MS spectra. In previous studies on mAF4-ESI-MS/MS,[33,36] the outflow of mAF4 was split from 16 to 6 μL/min using an additional syringe pump in the unpump mode, such that the total feed rate to MS was maintained at 11 μL/min after merging with the ionization modifier liquid. There were a few drawbacks during this flow split process, including loss of sample and inconsistent feed rate. However, the present study adopted splitless feeding of the mAF4 outflow (= 25 μL/min). After mixing with an ionization modifier liquid flow (= 25 μL/min), the total feed rate to MS was adjusted to 50 μL/min, and ESI was successful with the help of a HESI-II ion source along with the sheath gas (N_2). This resulted in an improvement in the consistent feed rate and thus stability in MS detection.

The direct detection of protein components from HDL and LDL by mAF4-ESI-MS/MS requires a further optimization of experimental conditions to increase the ionization efficiency because of their large MWs and the spectral congestion caused by abundant lipids. In this study, the proportion of organic solvents (ACN/MeOH, 5:5 in v/v) used for the ionization modifier liquid (1.0% formic acid in the positive ion mode and 0.5% ammonium hydroxide in the negative ion mode), which was merged with the aqueous outflow of mAF4 prior to ESI-MS, was varied to increase the ionization efficiency of protein components of the lipoprotein. Figure 3a shows the EIF of PC 34:2 from the HDL standard (2 μg) based on the SRM transition of m/z 758.5 → m/z 184.0 superimposed on the EIF of the CA standard (0.5 μg), which was obtained from the SRM transition of m/z 1001.5 ($[M + 29H]^{29+}$) → m/z 983.5

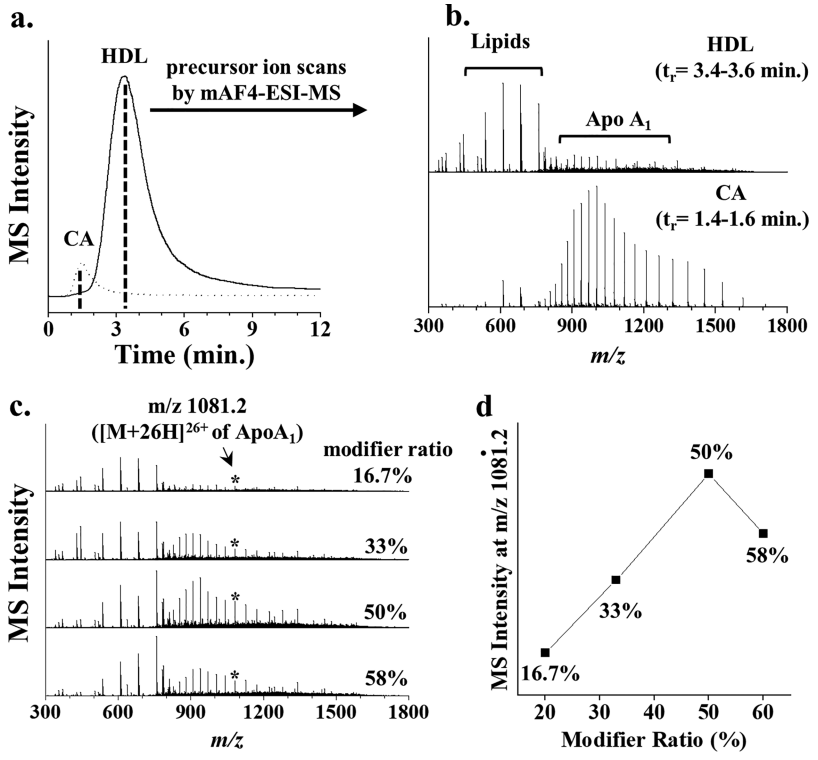

Figure 3. (a) EIF of PC 34:2 (SRM transition of m/z 758.5 → m/z 184.0) from the HDL standard superimposed on a fractogram of CA as an IS (0.5 μg) obtained by mAF4-ESI-MS/MS, (b) MS spectra of HDL (t_r = 3.4−3.6 min) and CA (t_r = 1.4−1.6 min) in positive ion mode, (c) MS spectra of HDL obtained at different compositions of the ionization modifier in the final feed to MS, and (d) effect of ionization modifier composition on the MS intensity of $[M + 26H]^{26+}$ of ApoA1 at m/z 1081.2.

https://dx.doi.org/10.1021/acs.analchem.0c04756
Anal. Chem. 2021, 93, 4867−4875

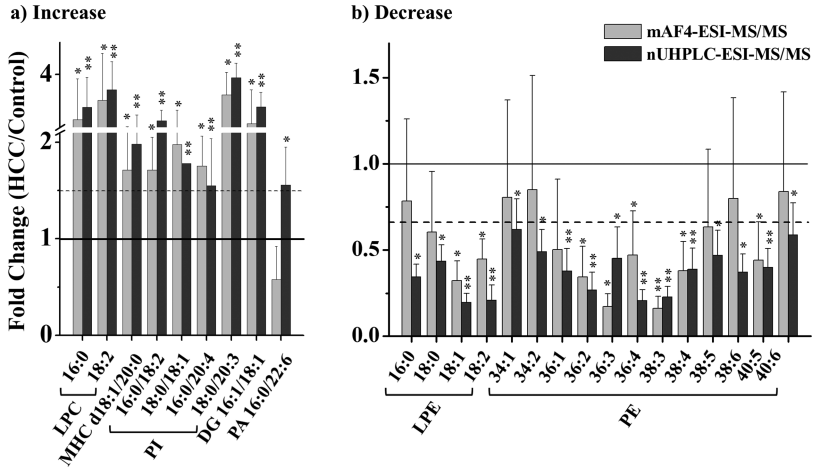

Figure 4. Bar graphs representing the calculated fold changes (HCC/control) of (a) 9 increased and (b) 16 decreased lipid targets from patients' plasma in comparison with healthy controls obtained by mAF4-ESI-MS/MS and nUPLC-ESI-MS/MS (* for $p < 0.05$; ** for $p < 0.01$).

(y_{69}^{8+}), the multiply charged peptide fragment ion. The MS spectra of the HDL fraction during the time interval t_r = 3.4–3.6 min showed a number of peaks from lipids and ApoA1 (Figure 3b), whereas the MS spectra of the CA fraction during t_r = 1.4–1.6 min showed multiply charged protein ions with larger peak intensities compared to the weak signals of ApoA1, although both proteins are similar in their molar mass values (ApoA1, 30 K; CA, 29 K). This indicates that the ionization of ApoA1 was suppressed by other lipids present in lipoproteins. To enhance the ionization of ApoA1, the amount of organic solvents in the total feed flow (ionization modifier liquid plus mAF4 effluent) was adjusted to enhance the dissociation of lipoprotein particles when they were fed to ESI-MS. Figure 3c shows the comparison of the peak intensities of m/z 1081.2 ($[M + 26H]^{26+}$), ApoA1 precursor ion, by varying the flow rate of the ionization modifier liquid from 5 to 35 μL/min using a syringe pump, whereas the outflow rate of mAF4 was fixed at 25 μL/min. Accordingly, the composition of the ionization modifier organic solvent in the final flow fed to MS gradually increased from 16.7 to 58.3%. As the composition of the ionization modifier organic solvent increased from 16.7%, the MS intensity of the ion $[M + 26H]^{26+}$ of ApoA1 increased up to 50% (50 μL/min of the total feed rate) but decreased with a further increase of the organic content to 58.3% (Figure 3d). As the proportion of organic solvent increased, the ionization efficiency of ApoA1 increased relatively with the increased dissociation of lipoprotein particles; however, the ESI efficiency decreased because of the increase in the final feed rate to MS (60 μL/min for 58.3%). This shows that the proportion of organic solvent in the final feed significantly influenced the ionization efficiency of ApoA1 during the mAF4-ESI-MS/MS analysis of lipoproteins, and 50% organic solvent was used for further analysis.

The high-speed screening capability of mAF4-ESI-MS/MS for lipoprotein components was evaluated using plasma samples from patients with HCC, and the results were compared with those obtained using nUHPLC-ESI-MS/MS. For quantitative analysis using mAF4-ESI-MS/MS, CA was added to the plasma sample as an IS (500 ng per 10 μL injection of each depleted plasma sample) to compensate for the run-to-run spectral fluctuations, and quantified lipid species were expressed as the relative ratio of the total peak area of lipoprotein (both HDL and LDL) to that of CA. In an earlier study on the lipidomic comparison of plasma samples from patients with five different cancers, including HCC, using nUHPLC-ESI-MS/MS,[31] the plasma lipid profiles of patients with HCC were compared with those of healthy controls and 25 lipid molecules (2 LPC, 4 LPE, 12 PE, 1 DG, 1 HexCer, 1 PA, and 4 PI), showing a significant difference (greater than twofold, and p value < 0.01) in patients with HCC that were identified as candidate markers. The reported molecules were adopted as target lipids for quantification using mAF4-ESI-MS/MS and confirmation using nUHPLC-ESI-MS/MS in this study. For nUHPLC-ESI-MS/MS analysis, lipid extraction was carried out with each plasma sample, and lipid species from individual lipid extract samples were quantified by calculating the corrected peak area, which is the ratio of the measured peak areas of the target species to that of each IS (1 pmol of each injection) corresponding to each lipid class, added to the lipid extract sample. Individual lipid levels of the healthy controls and HCC patients obtained by the two analytical methods were compared using a heat map (Figure S2). Most target lipids showed the same increasing or decreasing trends in patients with HCC by both mAF4-ESI-MS/MS and nUHPLC-ESI-MS/MS methods: the contents of LPC, DG, and PI species were significantly increased in HCC, whereas the contents of all the targeted LPE and PE species were significantly decreased. An exception was PA 16:0/22:6, which showed opposite results. Eight species were found to increase by more than 50% in the patient group (Figure 4a), and all PEs including LPEs decreased by more than 50% (dotted line) in the patient group (Figure 4b). Statistical comparison of the results from the two analytical methods (mAF4-ESI-MS/MS and nUHPLC-ESI-MS/MS) was performed using a paired t test by utilizing the fold ratio values of the 25 target lipids from 10 individual patient samples. Calculation of the fold ratio of individual lipids for each patient sample was based on the use of the average peak area of the control group. The calculated p values for all patients were larger than 0.05 (Table S3), implying that the results from the two analytical approaches were not significantly different from each other. This supports the conclusion that mAF4-ESI-MS/MS can be utilized as a high-speed screening device for the top-down analysis of plasma lipids. In addition, mAF4-ESI-MS/MS offers advantages such as fast analysis of intact lipoprotein components,

https://dx.doi.org/10.1021/acs.analchem.0c04756
Anal. Chem. 2021, 93, 4867–4875

removal of lipid extraction process, and online desalting during mAF4 runs.

The mAF4-ESI-MS/MS method offers a selected analysis of target species in either HDL or LDL particles. Figure 5 shows

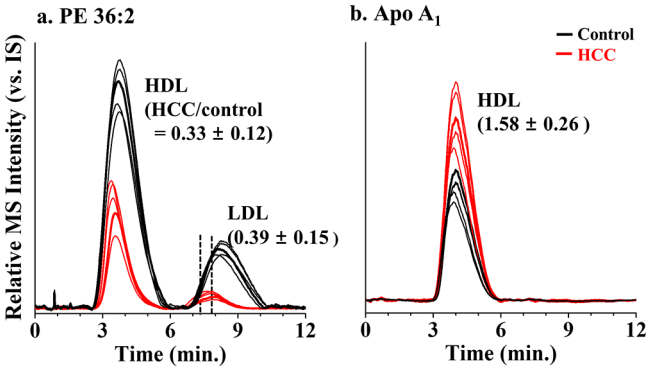

Figure 5. EIFs of plasma samples from patients with HCC (red, n = 10) and controls (black, n = 10) based on the detection of (a) PE 36:2 (SRM transition of m/z 744.5 → m/z 603.5) and (b) ApoA1 (SRM transition of m/z 1081.2 → m/z 864.3).

the superimposed MS signals of (a) PE 36:2 based on the SRM transition of m/z 744.5 → m/z 603.5 ($[M + H\text{-}141]^+$) and (b) ApoA1 based on the SRM transition of m/z 1081.2 ($[M + 26H]^{26+}$) → m/z 864.3 (y_{178}^{24+}) from individual plasma samples (10 HCC patients in red and 10 controls in black) obtained by mAF4-ESI-MS/MS under the same run conditions used in Figure 3. We showed a clear difference in the relative amount of PE 36:2 between HDL and LDL particles and a significant difference in its amounts between the HCC and control groups (Figure 5). The average peak area ratio of HCC samples to control samples (HCC/control) for PE 36:2 decreased to 0.33 ± 0.12 in HDL and 0.39 ± 0.15 in LDL (n = 10) (Figure 5a). Moreover, SRM fractograms show some decrease in the average retention time (t_r = 7.83 ± 0.12 min) of LDL particles in HCC patient samples compared with controls (t_r = 8.02 ± 0.10 min) (Figure 5a). This suggests a size reduction of LDL particles in the plasma of HCC patients. A decrease in the LDL particle size is typically found in the plasma of patients with cardiovascular diseases, such as CAD. Using mAF4-ESI-MS/MS for sample analysis is advantageous as it allows the simultaneous analysis of the lipid and protein components of the lipoproteins using a top-down approach. EIFs of ApoA1 were compared between individual control and HCC samples (Figure 5b). As ApoA1 is a major structural protein component of HDL and is rarely present in other lipoproteins, it was exclusively detected in HDL in both the control and patient groups. Previous studies have revealed that the ApoA1 concentration increased in the blood of HCC patients, which could be an unfavorable prognosis.[37,38] In our study, the fold ratio (HCC/control) of the ApoA1 peak area was calculated as 1.58 ± 0.26 (n = 10), demonstrating that the relative quantification of the protein component of lipoproteins can be accomplished at a high speed (<6 min) using mAF4-ESI-MS/MS without undergoing a complicated bottom-up proteomic analysis including protein digestion and LC−MS/MS analysis.

Results from other target lipids (LPC 18:2, PE 36:3, PA 18:1/18:1, and PI 18:0/20:3) showed a characteristic feature of the top-down lipid analysis with mAF4-ESI-MS/MS, revealing that not all lipid species have the same decreasing or increasing pattern in both lipoproteins (Figure 6a). Although the LPC 18:2 species were increased in both HDL

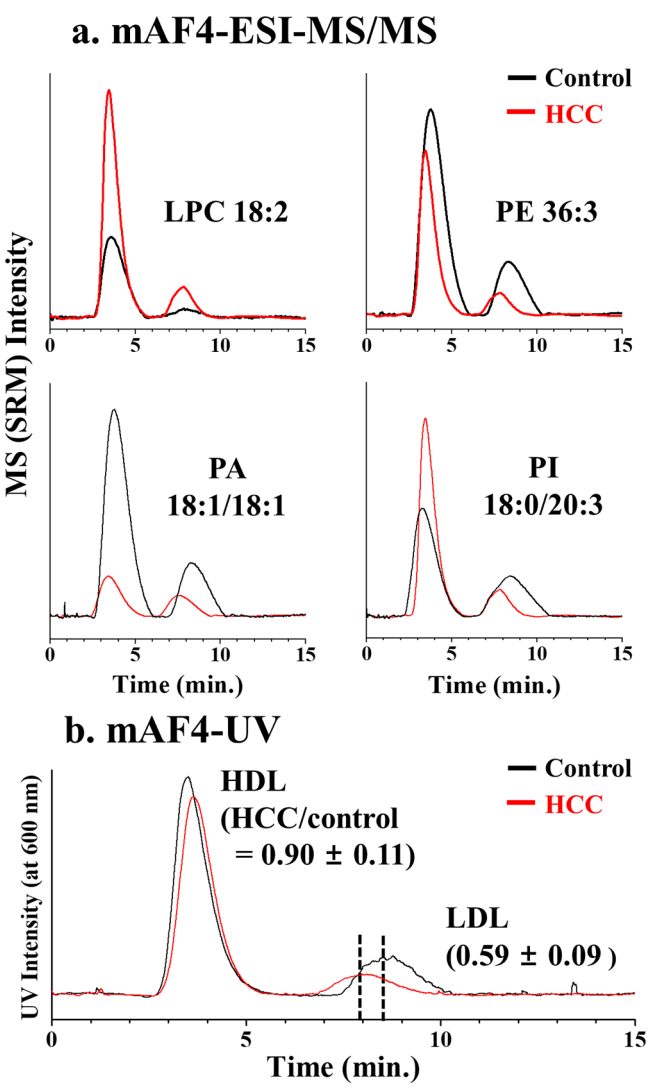

Figure 6. (a) EIFs of plasma samples based on the SRM transition of LPC 18:2 (m/z 520.5 → m/z 184.0), PE 36:3 (m/z 742.5 → m/z 601.5), PA 18:1/18:1 (m/z 699.5 → m/z 283.3), and PI 18:0/20:3 (m/z 887.5 → m/z 383.3) by mAF4-ESI-MS/MS for comparison between the control and HCC groups of plasma samples and (b) mAF4-UV fractogram of each pooled plasma sample from HCC patients and controls.

and LDL in the patient sample, PE 36:3 and PA 18:1/18:1 appeared to decrease in both HDL and LDL of liver cancer samples; however, PA18:1/18:1 decreased much more in HDL than in LDL. Moreover, PI 18:0/20:3 showed an opposite pattern where its level in the HCC group increased in HDL but decreased in LDL, and the overall level was increased. These results indicate that, in addition to the shrinkage of LDL during HCC pathogenesis, the lipid composition of each lipoprotein particle also changes.

The fold ratios of the 25 selected lipids and ApoA1, as analyzed by mAF4-ESI-MS/MS, are listed in Table 1 and compared with the values obtained using nUHPLC-ESI-MS/MS. The fold ratio values from mAF4-ESI-MS/MS were represented at both lipoprotein levels (HDL and LDL separately) and at the overall level (combined HDL and

https://dx.doi.org/10.1021/acs.analchem.0c04756
Anal. Chem. 2021, 93, 4867−4875

Table 1. Comparison of Calculated Fold Ratios (HCC/Control, n = 10 Each) for 25 Targeted Lipids and ApoA1 in Plasma Samples between mAF4-ESI-MS/MS and nUHPLC-ESI-MS/MS (* for $p < 0.05$, ** for $p < 0.01$)

			HCC/control			
			mAF4-ESI-MS/MS			
species	acyl chain	m/z	HDL	LDL	overall	nUPLC-ESI-MS/MS
LPC	16:0	496.5	1.53 ± 0.81*	5.30 ± 1.21**	2.47 ± 1.39*	2.89 ± 1.02**
	18:2	520.5	2.04 ± 0.97**	6.41 ± 1.52**	3.12 ± 1.60*	3.49 ± 0.95**
LPE	16:0	454.5	0.78 ± 0.29	0.81 ± 0.39	0.79 ± 0.47	0.34 ± 0.07*
	18:0	482.5	0.57 ± 0.30**	0.68 ± 0.22*	0.60 ± 0.35	0.43 ± 0.09*
	18:1	480.5	0.32 ± 0.07**	0.31 ± 0.09**	0.32 ± 0.11*	0.20 ± 0.05**
	18:2	478.5	0.43 ± 0.10**	0.51 ± 0.21**	0.45 ± 0.21*	0.21 ± 0.09**
PE	34:1	718.5	0.83 ± 0.41	0.74 ± 0.39	0.80 ± 0.57	0.62 ± 0.18*
	34:2	716.5	0.91 ± 0.62	0.67 ± 0.29*	0.85 ± 0.66	0.49 ± 0.13*
	36:1	746.5	0.53 ± 0.32*	0.43 ± 0.28*	0.50 ± 0.41	0.38 ± 0.11**
	36:2	744.5	0.33 ± 0.12**	0.39 ± 0.15*	0.34 ± 0.18*	0.27 ± 0.10**
	36:3	742.5	0.18 ± 0.05**	0.17 ± 0.05**	0.17 ± 0.07*	0.45 ± 0.18*
	36:4	740.5	0.46 ± 0.12**	0.51 ± 0.25**	0.47 ± 0.26*	0.21 ± 0.06**
	38:3	770.5	0.14 ± 0.05**	0.21 ± 0.07**	0.16 ± 0.07**	0.23 ± 0.06**
	38:4	768.5	0.31 ± 0.10**	0.57 ± 0.21*	0.38 ± 0.17*	0.39 ± 0.12**
	38:5	766.5	0.63 ± 0.40*	0.64 ± 0.31*	0.63 ± 0.45	0.47 ± 0.14*
	38:6	764.5	0.81 ± 0.62	0.76 ± 0.29*	0.80 ± 0.58	0.37 ± 0.11*
	40:5	794.5	0.36 ± 0.13**	0.69 ± 0.29	0.44 ± 0.22*	0.40 ± 0.11**
	40:6	792.5	0.83 ± 0.42	0.89 ± 0.49	0.84 ± 0.58	0.59 ± 0.19*
DG	16:1,18:0	612.5	2.53 ± 0.94*	1.75 ± 0.66*	2.33 ± 1.20*	2.89 ± 0.52**
HexCer	d18:1/20:0	800.5	1.95 ± 0.54*	0.98 ± 0.21	1.71 ± 0.52*	1.98 ± 0.64**
PA	16:0/22:6	719.5	0.46 ± 0.12*	0.51 ± 0.25	0.58 ± 0.34	1.56 ± 0.39*
PI	16:0/20:4	857.5	2.03 ± 0.38**	0.93 ± 0.09	1.76 ± 0.31*	1.55 ± 0.48**
	18:0/20:3	887.5	4.40 ± 0.40**	0.20 ± 0.05**	3.30 ± 0.87*	3.89 ± 0.50**
	18:1/18:0	863.5	2.13 ± 0.54**	1.55 ± 0.60*	1.98 ± 0.89*	1.78 ± 0.39**
	16:0/18:2	835.5	1.83 ± 0.24**	1.35 ± 0.20*	1.71 ± 0.34*	2.42 ± 0.37**
ApoA1		1081.2	1.58 ± 0.26*			

LDL results). The plasma levels of all selected LPE and PE species were significantly decreased in HCC patients. As PE is the second-most abundant phospholipid in mitochondria, which are abundant in liver cells, the levels of PE in HCC could be significantly lowered because of the damage to liver cells. A previous study by Chen et al.[39] showed that PEs were significantly reduced in the serum of HCC patients compared to healthy controls, which is consistent with our results. However, the PE levels were found to decrease in multiple cancers (liver, gastric, lung, and colorectal);[31] therefore, its decrease was not unique to HCC. HexCer d18:1/20:0 was upregulated in patients with HCC,[40] similar to the observation in our study. LPC is known to act as a proinflammatory mediator, especially saturated LPC,[41] and is considered to be associated with cancer metastasis.[42,43] In our study, the two targeted LPCs (16:0 and 18:2) were significantly upregulated in HCC patients (more than twofold). More importantly, four PI species and DG 16:1/18:1 among the 25 selected species were identified in an earlier study to be unique biomarker candidates for HCC among five cancers, whereas the contents of two LPCs (16:0 and 18:2) and HexCer d18:1/20:0 were commonly increased in gastric cancer and lung cancer, respectively, in addition to HCC.[31] The present study demonstrated the capability of mAF4-ESI-MS/MS in successfully differentiating HCC-specific lipid species (four PIs and DG 16:1/18:1) along with few other signature molecules.

The liver is the main organ for energy metabolism, and most plasma apolipoproteins, endogenous lipids, and lipoproteins are synthesized in the liver. Under the development of HCC, the homeostasis of lipids and lipoprotein metabolism are impaired, leading to alterations in the plasma lipid composition and the relative amount of lipoproteins.[44] In particular, a number of studies reported that plasma LDL levels were reduced in the HCC group more than that in controls.[45−47] In our study, the total level of LDL was not measured, but most lipid species of LDL, including PC, which is the most abundant phospholipid, decreased in the HCC group. According to the UV signals of mAF4 separation of each pooled plasma sample from patients and controls (Figure 6b), the LDL peak was significantly reduced by more than 40% (n = 3) compared with that of controls. Typically, the LDL size decreases with the increase of its level in patients with CAD[18,48] and postmenopausal osteoporosis.[49] This is an outstanding feature of FlFFF in determining the size reduction and level change of LDL simultaneously.

CONCLUSIONS

In this study, the mAF4 run condition was optimized to achieve a baseline separation of HDL and LDL within 10 min for the high-speed screening of lipoprotein components from plasma samples, and the proportion of organic solvents in the ionization modifier liquid was optimized to increase the ionization efficiency of protein components of lipoproteins. Targeted analysis of lipoprotein components from human plasma samples was then conducted to elucidate the alteration in the composition of lipoproteins affected by HCC development using mAF4-ESI-MS/MS. This study was focused on the top-down targeted quantification of lipid biomarker candidates that exhibited significant differences in patients with HCC in a previous report[31] by using mAF4-ESI-MS/MS. Among the 25

https://dx.doi.org/10.1021/acs.analchem.0c04756
Anal. Chem. 2021, 93, 4867−4875

targeted lipid species examined by mAF4-ESI-MS/MS, eight species (two LPC, four PI, one DG, and one HexCer) showed significant increases of more than 50% in HCC patients, and all LPE and PE species (4 LPE and 12 PE) decreased by more than 50% in the patient group. Target lipids from the same plasma samples were also analyzed by nUHPLC-ESI-MS/MS by bottom-up lipidomic analysis for statistical comparison with the results from mAF4-ESI-MS/MS, showing that the results were not statistically different. In addition to lipid analysis, the top-down analysis of ApoA1, which is an important protein component of lipoproteins, could be accomplished by mAF4-ESI-MS/MS, showing that ApoA1 was increased by more than 50% in patients with HCC. Moreover, as mAF4 can fractionate different lipoproteins (HDL and LDL) by size, a decrease in the retention time of LDL peak in patients in comparison with controls can be monitored to distinguish the size reduction of LDL in HCC patients. This suggests that the present top-down analytical platform can provide not only the compositional analysis of lipoprotein changes but also the size and the relative amount of LDL in the plasma of patients with HCC. Selective quantification of both targeted lipids and ApoA1 without isolating ApoA1 from plasma proteins offers a great capability to be integrated as a high-speed analytical tool. As the present study showed the high-speed screening capability of mAF4-ESI-MS/MS for the candidate markers, it will be promising to develop a simple screening protocol for the diagnosis of HCC and other diseases involved with the perturbation in lipoproteins, such as cardiovascular diseases, using only a few drops of blood sample. The present method needs to be further investigated with a large number of samples from various diseases in order to integrate the developed method into a high-speed screening platform with the purpose of diagnosis. For this, an automation of mAF4 will be needed for the high-throughput analysis, and a possible carryover problem should be considered for the clinical usage. The carryover issue can be minimized with the use of a miniaturized hollow fiber FlFFF (mHF5) as an alternative FlFFF channel to mAF4 as the hollow fiber can be used as a disposable channel.

■ ASSOCIATED CONTENT

Supporting Information

The Supporting Information is available free of charge at https://pubs.acs.org/doi/10.1021/acs.analchem.0c04756.

Assembly of mAF4; lipid extraction from plasma samples by the modified MTBE/MeOH method; BPCs of lipid extracts from the plasma of control and HCC patient group in positive ion and negative ion modes of nUPLC-ESI-MS/MS; heatmap of total 41 targeted lipids from plasma samples between the control and HCC group using mAF4-ESI-MS/MS and nLC-ESI-MS/MS; demographic data for controls and liver cancer patient group; type of precursor ion, quantifier ion, and ionization mode used for each targeted lipid and protein species for SRM quantification by mAF4-ESI-MS/MS and nUHPLC-ESI-MS/MS; p values calculated using a paired t test to compare significant differences in the quantification of lipids between the nLC-ESI-MS/MS and mAF4-ESI-MS/MS methods (PDF)

■ AUTHOR INFORMATION

Corresponding Author

Myeong Hee Moon − *Department of Chemistry, Yonsei University, Seoul 03722, Republic of Korea;* orcid.org/0000-0002-5454-2601; Phone: (82) 2 2123 5634; Email: mhmoon@yonsei.ac.kr; Fax: (82) 2 364 7050

Authors

Jin Yong Kim − *Department of Chemistry, Yonsei University, Seoul 03722, Republic of Korea*

Gwang Bin Lee − *Department of Chemistry, Yonsei University, Seoul 03722, Republic of Korea*

Jong Cheol Lee − *Department of Chemistry, Yonsei University, Seoul 03722, Republic of Korea*

Complete contact information is available at: https://pubs.acs.org/10.1021/acs.analchem.0c04756

Notes

The authors declare no competing financial interest.

■ ACKNOWLEDGMENTS

This research was supported by the Basic Science Research Program through the National Research Foundation of Korea (NRF) funded by the Ministry of Education (NRF-2019R1A6A3A01094710) and in part by a grant (NRF2018R1A2A1A05019794) of the Ministry of Science, ICT & Future Planning through the NRF.

■ REFERENCES

(1) Shevchenko, A.; Simons, K. *Nat. Rev. Mol. Cell Biol.* **2010**, *11*, 593−598.
(2) Wenk, M. R. *Cell* **2010**, *143*, 888−895.
(3) Holthuis, J. C. M.; Menon, A. K. *Nature* **2014**, *510*, 48−57.
(4) Wymann, M. P.; Schneiter, R. *Nat. Rev. Mol. Cell Biol.* **2008**, *9*, 162−176.
(5) Wong, L. H.; Čopič, A.; Levine, T. P. *Trends Biochem. Sci.* **2017**, *42*, 516−530.
(6) Bruce, C.; Chouinard, R. A., Jr; Tall, A. R. *Annu. Rev. Nutr.* **1998**, *18*, 297−330.
(7) von Zychlinski, A.; Williams, M.; McCormick, S.; Kleffmann, T. *J. Proteomics* **2014**, *106*, 181−190.
(8) Meshkani, R.; Adeli, K. *Clin. Biochem.* **2009**, *42*, 1331−1346.
(9) Haghikia, A.; Landmesser, U. *Antioxid. Redox Signaling* **2018**, *29*, 337−352.
(10) Borgquist, S.; Butt, T.; Almgren, P.; Shiffman, D.; Stocks, T.; Orho-Melander, M.; Manjer, J.; Melander, O. *Int. J. Cancer* **2016**, *138*, 2648−2656.
(11) Ren, L.; Yi, J.; Li, W.; Zheng, X.; Liu, J.; Wang, J.; Du, G. *Cancer Med.* **2019**, *8*, 7032−7043.
(12) Paapstel, K.; Kals, J.; Eha, J.; Tootsi, K.; Ottas, A.; Piir, A.; Jakobson, M.; Lieberg, J.; Zilmer, M. *Nutr., Metab. Cardiovasc. Dis.* **2018**, *28*, 44−52.
(13) Griffin, B. A.; Caslake, M. J.; Yip, B.; Tait, G. W.; Packard, C. J.; Shepherd, J. *Atherosclerosis* **1990**, *83*, 59−67.
(14) Dernick, G.; Obermüller, S.; Mangold, C.; Magg, C.; Matile, H.; Gutmann, O.; von der Mark, E.; Handschin, C.; Maugeais, C.; Niesor, E. J. *J. Lipid Res.* **2011**, *52*, 2323−2331.
(15) Pérusse, M.; Pascot, A.; Després, J.-P.; Couillard, C.; Lamarche, B. *J. Lipid Res.* **2001**, *42*, 1331−1334.
(16) Osei, M.; Griffin, J. L.; Koulman, A. *Rapid Commun. Mass Spectrom.* **2015**, *29*, 1969−1976.
(17) Lee, H.; Williams, S. K. R.; Wahl, K. L.; Valentine, N. B. *Anal. Chem.* **2003**, *75*, 2746−2752.
(18) Rambaldi, D. C.; Zattoni, A.; Casolari, S.; Reschiglian, P.; Roessner, D.; Johann, C. *Clin. Chem.* **2007**, *53*, 2026−2029.

(19) Kang, D.; Oh, S.; Reschiglian, P.; Moon, M. H. *Analyst* **2008**, *133*, 505−515.
(20) Kim, J. Y.; Kim, S.-K.; Kang, D.; Moon, M. H. *Anal. Chem.* **2012**, *84*, 5343−5350.
(21) Yang, J. S.; Lee, J. Y.; Moon, M. H. *Anal. Chem.* **2015**, *87*, 6342−6348.
(22) Rambaldi, D. C.; Reschiglian, P.; Zattoni, A.; Johann, C. *Anal. Chim. Acta* **2009**, *654*, 64−70.
(23) Bria, C. R. M.; Afshinnia, F.; Skelly, P. W.; Rajendiran, T. M.; Kayampilly, P.; Thomas, T. P.; Andreev, V. P.; Pennathur, S.; Kim Ratanathanawongs Williams, S. *Anal. Bioanal. Chem.* **2019**, *411*, 777−786.
(24) Giddings, J. C. *Anal. Chem.* **1981**, *53*, 1170A−1178A.
(25) Giddings, J. *Science* **1993**, *260*, 1456−1465.
(26) Moon, M. H. *TrAC, Trends Anal. Chem.* **2019**, *118*, 19−28.
(27) Byeon, S. K.; Kim, J. Y.; Lee, J. Y.; Chung, B. C.; Seo, H. S.; Moon, M. H. *J. Chromatogr. A* **2015**, *1405*, 140−148.
(28) Kim, J. Y.; Lim, H. B.; Moon, M. H. *Anal. Chem.* **2016**, *88*, 10198−10205.
(29) Reschiglian, P.; Zattoni, A.; Roda, B.; Cinque, L.; Parisi, D.; Roda, A.; Dal Piaz, F.; Moon, M. H.; Min, B. R. *Anal. Chem.* **2005**, *77*, 47−56.
(30) Kourtchev, I.; Szeto, P.; O'Connor, I.; Popoola, O. A. M.; Maenhaut, W.; Wenger, J.; Kalberer, M. *Anal. Chem.* **2020**, *92*, 8396−8403.
(31) Lee, G. B.; Lee, J. C.; Moon, M. H. *Anal. Chim. Acta* **2019**, *1063*, 117−126.
(32) Ishikawa, M.; Maekawa, K.; Saito, K.; Senoo, Y.; Urata, M.; Murayama, M.; Tajima, Y.; Kumagai, Y.; Saito, Y. *PLoS One* **2014**, *9*, No. e91806.
(33) Yang, I.; Kim, K. H.; Lee, J. Y.; Moon, M. H. *J. Chromatogr. A* **2014**, *1324*, 224−230.
(34) Byeon, S. K.; Lee, J. Y.; Moon, M. H. *Analyst* **2012**, *137*, 451−458.
(35) Byeon, S. K.; Lee, J. Y.; Lee, J.-S.; Moon, M. H. *J. Chromatogr. A* **2015**, *1381*, 132−139.
(36) Kim, K. H.; Lee, J. Y.; Lim, S.; Moon, M. H. *J. Chromatogr. A* **2013**, *1280*, 92−97.
(37) Ma, X.-L.; Gao, X.-H.; Gong, Z.-J.; Wu, J.; Tian, L.; Zhang, C.-Y.; Zhou, Y.; Sun, Y.-F.; Hu, B.; Qiu, S.-j.; Zhou, J.; Fan, J.; Guo, W.; Yang, X.-R. *Oncotarget* **2016**, *7*, 70654.
(38) Bharali, D.; Banerjee, B. D.; Bharadwaj, M.; Husain, S. A.; Kar, P. *Indian J. Med. Res.* **2018**, *147*, 361.
(39) Lu, Y.; Chen, J.; Huang, C.; Li, N.; Zou, L.; Chia, S. E.; Chen, S.; Yu, K.; Ling, Q.; Cheng, Q.; Zhu, M.; Zhang, W.; Chen, M.; Ong, C. N. *Oncotarget* **2018**, *9*, 5032.
(40) Li, J.; Hu, C.; Zhao, X.; Dai, W.; Chen, S.; Lu, X.; Xu, G. *J. Chromatogr. A* **2013**, *1320*, 103−110.
(41) del Bas, J. M.; Caimari, A.; Rodriguez-Naranjo, M. I.; Childs, C. E.; Paras Chavez, C.; West, A. L.; Miles, E. A.; Arola, L.; Calder, P. C. *Am. J. Clin. Nutr.* **2016**, *104*, 266−279.
(42) Fukushima, N.; Ishii, I.; Contos, J. J.; Weiner, J. A.; Chun, J. *Annu. Rev. Pharmacol. Toxicol.* **2001**, *41*, 507−534.
(43) Jantscheff, P.; Schlesinger, M.; Fritzsche, J.; Taylor, L. A.; Graeser, R.; Kirfel, G.; Fürst, D. O.; Massing, U.; Bendas, G. *Mol. Cancer Ther.* **2011**, *10*, 186−197.
(44) Jiang, J.; Nilsson-Ehle, P.; Xu, N. *Lipids Health Dis.* **2006**, *5*, 4.
(45) Lewis, G. F.; Rader, D. J. *Circ. Res.* **2005**, *96*, 1221−1232.
(46) Ooi, K.; Shiraki, K.; Sakurai, Y.; Morishita, Y.; Nobori, T. *Int. J. Mol. Med.* **2005**, *15*, 655−660.
(47) Chen, Y.; Zhou, J.; Li, J.; Feng, J.; Chen, Z.; Wang, X. *Oncotarget* **2016**, *7*, 47332.
(48) Park, I.; Paeng, K.-J.; Yoon, Y.; Song, J.-H.; Moon, M. H. *J. Chromatogr. B: Biomed. Sci. Appl.* **2002**, *780*, 415−422.
(49) Lee, K. G.; Lee, G. B.; Yang, J. S.; Moon, M. H. *Antioxidants* **2020**, *9*, 46.

https://dx.doi.org/10.1021/acs.analchem.0c04756
Anal. Chem. 2021, 93, 4867−4875